JOURNAL OF PROPULSION AND POWER
Vol. 18, No. 5, September–October 2002

Combustion Response of Ammonium Perchlorate Composite Propellants

Michael Shusser* and Fred E. C. Culick†
California Institute of Technology, Pasadena, California 91125
and
Norman S. Cohen‡
Cohen Professional Services, Redlands, California 92373

The Cohen and Strand model for ammonium perchlorate (AP) composite propellants is applied as boundary conditions, one for AP and one for binder, in solving the heat conduction equation in each to compute linear and nonlinear combustion response properties for each and for the aggregate propellant. Iterations couple AP and binder through the quasi-steady flame processes. Illustrative results for linear response functions (pressure coupled and velocity coupled) are presented for a monomodal AP propellant showing effects of varying AP size, pressure, and crossflow speed. Examples of nonlinear responses to arbitrary waveforms are also shown. The model predicts a very large response at high pressures with coarse AP due to AP monopropellant combustion, underpredicts peak response amplitude for low pressures due to a possible change in mechanism, and shows a stabilizing effect of the diffusion flame. A quantitative comparison with response function data is limited to one well-characterized research formulation. Mechanistic implications are discussed, including recommendations for future modeling work.

Nomenclature

a	=	steady-state speed of sound
H_c	=	dimensionless net heat release in the condensed phase of the ammonium perchlorate (AP)
H_f	=	dimensionless heat of decomposition of the binder
H_{ox}	=	dimensionless heat release in the AP flame
H_{PF}	=	dimensionless heat release in the diffusion flame (with reference to the AP heat balance)
$H_{PF\,f}$	=	analogous to H_{PF} but with reference to the binder heat balance
m_i	=	mass flux
P	=	dimensionless pressure, when equal to 1 is steady-state
Q_{ox}	=	dimensional H_{ox}
Q_L	=	dimensional condensed-phase heat release in the AP
Q_{PF}	=	dimensional H_{PF} or $H_{PF\,f}$, has the same dimensional value
R	=	dimensionless propellant burning rate, when equal to 1, is steady state
R_f	=	dimensionless binder burning rate
R_{ox}	=	dimensionless AP burning rate
R_{pc}	=	pressure-coupled response function
R_{vc}	=	velocity-coupled response function
S_i	=	fraction of propellant surface area occupied by ith ingredient
T_{Si}	=	surface temperature of ith ingredient
u'	=	crossflow velocity perturbation, dimensional
V	=	dimensionless crossflow speed, when equal to 1, is steady state if >0
X^*_{ox}	=	AP flame height
X^*_{PDF}	=	diffusion flame height
z_i	=	dimensionless distance into the solid phase of ith ingredient
α_{ox}	=	fraction of propellant mass flow rate from the AP, wt% AP in steady state
β_F	=	fraction of AP that goes to the diffusion flame, rest goes to the AP flame
β_{ox}	=	fraction of diffusion flame energy that heats the AP, rest heats the binder
β_p	=	fraction of AP heat release that occurs in the flame, rest occurs in condensed phase
ε_i	=	dimensionless semi-empirical convection term added to the energy balance for crossflow
θ_i	=	dimensionless temperature difference (from the initial temperature)
ξ_i	=	dimensionless flame heights
ρ_i	=	ingredient or propellant density
τ	=	dimensionless time step ($\frac{1}{40}$ of the period of the imposed wave)
Ω_i	=	dimensionless frequency

Subscripts

f	=	binder
ox	=	AP
PF	=	portion of diffusion flame over AP
PFf	=	portion of diffusion flame over binder
p	=	aggregate propellant

Received 1 April 2001; revision received 28 April 2002; accepted for publication 30 April 2002.

*Postdoctoral Scholar, Mechanical Engineering. Member AIAA.
†Richard L and Dorothy M Professor, Mechanical Engineering and Jet Propulsion. Fellow AIAA.
‡Subcontractor. Associate Fellow AIAA.

Introduction

THE main objective of combustion instability studies is to develop the understanding and capabilities that will assure the stability of future solid rocket motors employing advanced propellants. A starting point is to work with ammonium perchlorate (AP) composite propellants because of their long history and continuing interest for the foreseeable future. Furthermore, the axial mode instabilities of motors containing AP composite propellants present the most challenging instability problem. The most frequent encounters with axial mode instabilities are with AP propellants, and the convenience of particle damping by additives to suppress high-frequency modes is not available at the lower axial mode frequencies. Moreover, the axial modes are associated with the important gasdynamic mechanism of vortex shedding.

The ultimate modeling goal is to achieve a numerical simulation of the internal flowfields of solid motors, which necessarily includes coupling the motor chamber gasdynamics with the combustion process at the boundaries of the flowfield. The standard work in this area has been the Baum and Levine nonlinear instability code,[1] which coupled one-dimensional gasdynamics with a simple and heuristic combustion model. Although remarkable in its ability to describe features of nonlinear instability observed in research motors, this code is inadequate to represent most geometries of practical interest, and its combustion model does not contain mechanisms to isolate key variables such as AP particle size and turbulence interaction. Thus, there is a need to evolve to two-dimensional gasdynamics coupled with a comprehensive composite propellant combustion model. The objective here is to develop a mechanistic AP propellant combustion model code that can be coupled with a two-dimensional gasdynamics code.

Recently, Knott and Brewster[2] and Hegab et al.[3] solved multidimensional versions of the heat equation with multiple components, coupled to a gas phase with a free-surface boundary condition. However, if one wants to couple combustion to gasdynamics, simpler models, such as the one used in the present study, have a distinct advantage.

Propellant Combustion Model

Background

The model being used in this work is the Cohen and Strand model.[4] It has already been used to explain effects of AP particle size, pressure, and crossflow on combustion response properties in a general way.[5,6] However, it has not yet been incorporated into a numerical scheme that would take full advantage of its mechanistic features.

A first step was to develop a nonlinear code for monopropellant AP. This was successfully accomplished[7] and made more useful by the acquisition of response function data for AP (Ref. 8). The model was in reasonable agreement with the data and provided mechanistic insights on the combustion response properties of AP: the roles of the surface decomposition law and the heat feedback law, the roles of exothermic condensed phase reactions vis-á-vis flame reactions, and intrinsic instability limits as possible explanations for the low-pressure deflagration limit P_{DL} of AP ($\sim$1.36 MPa) and for the unusual suppressed burning behavior exhibited by purified AP at very high pressures (>13.6 MPa). Based on this work, it was recommended that advanced energetic ingredients should release their energy primarily in the gas phase (minimal heat release in the condensed phase) and have low activation energies of decomposition to best promote combustion stability. It was more important that we learn something than have a working code or achieve good agreement with data.

The composite propellant model is well described in the original references[4–6] and will not be repeated here. For steady-state computations, the model accommodates trimodal AP size distributions. However, for the nonsteady computations, which are the subject of this work, it was restricted to monomodal AP for five basic reasons: 1) There is not general agreement as to how the various sizes contribute to coherent combustion response or to multipeaked response function curves often seen in propellant data. 2) The computational approach of obtaining coupled iterative solutions of the transient heat conduction equation for AP and binder would be too complicated for more than one AP size in the absence of agreed mechanistic justification. 3) To gain insights, it is prudent to begin by examining one size at a time. 4) It was of interest to see if the differing response properties of AP and binder, for example, different characteristic times, could be the reason for a dual-peaked response function curve. 5) The most extensive response function data in the literature are for monomodal AP research-type propellants. In addition, monodisperse (single particle size) models have been widely used to explain the mechanistic burning rate behavior of propellants.[9–11] Indeed, it turned out from the results obtained here that the way multimodal sizes contribute to steady-state combustion in the model may not be mechanistically correct, notwithstanding the ability of this and other similar steady-state models to predict burning rates (discussed later).

Procedure

As already noted, a key feature of the approach is to obtain solutions of the transient heat conduction equation in both the AP and binder as coupled through the flame processes. The heat conduction in propellants is assumed to be one dimensional. Lateral heat conduction between binder and AP in the condensed phase is neglected because its effect has been computed to be small.[12,13] Whereas AP and binder are constrained to preserve the propellant formulation (continuity) in steady state, they are free to vary independently in the course of oscillations such that compositional fluctuations arise; the propellant is preserved only as a time average over the oscillations. This produces a thermochemical fluctuation in the flame temperature as a response mechanism of potential importance. The need to account for compositional fluctuations had been proposed earlier by King[14] and Cohen and Strand[5] in connection with the differing response properties of AP and binder.

The computations for linear response functions begin with a steady-state computation that provides the initial conditions for AP and binder, including the respective solid-phase thermal profiles. A small perturbation sine wave is then imposed, typically 1% of the mean pressure. Strong responses (response function greater than about 5) require smaller perturbations to maintain linearity.[7]

The Crank–Nicholson numerical scheme is employed, with coordinate stretching to obtain finer grid near the solid surface (see Ref. 7 for more details). There are 201 mesh points, and the dimensionless time step is 0.001. A relatively high accuracy of computation is needed because Arrhenius kinetics yield small changes in the surface temperature.

In a two-component system such as a composite propellant, a double iteration is required for AP and binder because of their differing thermal wave properties. Although the boundary condition in the deep solid is the bulk temperature, the values of AP and binder surface temperatures are guessed in the iteration at each time step and used in the surface boundary condition for the heat conduction equation. For each component, heat flux at the surface is calculated using the temperature gradient at the surface and matched to the heat flux from the gas phase using the energy balance. The convergence criterion was 10^{-9}.

Both simultaneous and sequential solution procedures were examined. The simultaneous solution procedure makes new guesses for both AP and binder and iterates on both simultaneously, whereas the sequential procedure iterates the AP surface temperature until convergence for each new guess of the binder surface temperature. Both approaches agreed, inasmuch as the difference between the results was of the order of magnitude of the convergence criterion. This provided an additional check on the numerical scheme. However, from the standpoint of convergence speed, the sequential procedure was found to be clearly superior because it required several times less iterations. Therefore, it was used in calculations.

Initial work also involved study of detailed output to check for proper and consistent behavior of the parameters in the iteration steps and at the end of each time step in the course of the first oscillation, with special attention to the transition from the initial steady state to the unsteady; it all appeared to behave reasonably.

Boundary Conditions

The nonsteady boundary condition for the AP, from the composite propellant model, is

$$\left[\frac{\partial \theta_{ox}}{\partial z_{ox}}\right]_{gas} = R_{ox}\left[-H_c + \beta_{ox}(1-\beta_F)H_{ox}e^{-\xi_{ox}} + \beta_{ox}\beta_F\left(1+\frac{m_f S_f}{m_{ox}S_{ox}}\right)H_{PF}e^{-\xi_{PF}}\right] + \varepsilon_{ox} \tag{1}$$

and for the binder:

$$\left[\frac{\partial \theta_f}{\partial z_f}\right]_{gas} = R_f\left[-H_f + (1-\beta_{ox})\left(1+\frac{m_{ox}S_{ox}}{m_f S_f}\right)H_{PF\,f}e^{-\xi_{PF\,f}}\right] + \varepsilon_f \tag{2}$$

with $m_i = \rho_i r_i$, $m_p = m_{ox}S_{ox} + m_f S_f$ as $S_{ox} + S_f = 1$, $R_i = m_i/\bar{m}_i$.

The terms in the right-hand side of Eq. (1) correspond to condensed-phase reaction heat, heat feedback from the AP flame, heat feedback from the diffusion flame, and an erosive (crossflow) effect. The terms in the right-hand side of Eq. (2) are, respectively, condensed-phase reaction heat, diffusion flame heat feedback, and the analogous erosive effect. The forms of these terms come from the Cohen and Strand model,[4] which was selected for this study. When the model is coupled to the gasdynamics for motor stability analyses, the erosive burning heat feedback terms ε_i are replaced with Beddini's model as applied Ref. 15. In uncoupled studies of the combustion, there is no vehicle for incorporating the flowfield turbulence intensities and so the ε_i are retained to represent the effects of crossflow.

Results

Steady-State Checkout

The standard case for computations is 87% AP (20 μm) in hydroxyl-terminated-polybutadiene binder at 68 atm, zero crossflow. The steady-state model results at this condition are shown in Table 1. Previous work had shown that this condition provides maximum diffusion flame control and minimum pressure exponent in parametric model computations.[16,17] The diffusion flame is well inside the AP flame ($X^*_{\rm PDF} < X^*_{\rm ox}$) and is governed by its diffusion component. The surface is not planar because $S_{\rm ox}$ is closer to the AP weight fraction than to its volume fraction. About 48% of the AP ($1 - \beta_p$) reacts in the condensed phase, yielding a net exothermic condensed phase. (Negative Q_L is exothermic in the convention used.) All of the heat feedback from the gas phase is from the diffusion flame ($\beta_F = 1$), and the binder takes more than its share ($\beta_{\rm ox} <$ AP weight fraction). All of these results depend on particle size and pressure and are influenced by crossflow. Steady-state computations were performed as a preliminary step for each of the unsteady cases, which served as a check on the status of the Cohen and Strand[4] model within the nonsteady code.

Nonsteady Checkout

Table 2 shows the nonsteady results for this case at a dimensionless frequency of 7, referenced to the AP. The binder's dimensionless frequency is less than that for AP at a given dimensional frequency, and the aggregate propellant has yet another dimensionless frequency. The tabular results are solutions at each of the first 19 time increments, following the steady-state initial condition, which covers all but the last time step of the first half-cycle of the sinusoidal pressure wave.

This frequency happens to be close to the peak response frequencies for the propellant and the ingredients under this condition, and so the burning rates of the propellant and AP are in phase with the pressure. However, the binder slightly leads the pressure. One important observation in the detailed outputs was whether such phase shifts with pressure and between the AP and binder would appear. Over the ranges of Ω covered, examples of various phase shifts were encountered, and it was satisfying to see that. Here the binder leading causes an initial decrease in the fraction of mass flow from the AP, $\alpha_{\rm ox}$, and then an increase, which leads the pressure.

$Q_{\rm PF}$ has an interesting behavior, which is affected by competing processes. Whereas an initial decrease in $\alpha_{\rm ox}$ lowers the temperature, the companion increase in pressure eventually raises it. There results a wave behavior in $Q_{\rm PF}$ that is shifted from and distorted relative to the pressure wave. On the other hand, Q_L and its companion $Q_{\rm ox}$ are in phase with pressure and behave almost symmetrical with the pressure wave. The flame heights follow the pressure wave, as they should because the model assumes a quasi-steady gas phase. The change in the AP flame height is proportionally larger because it is kinetically controlled (pressure dependent), whereas the diffusion flame is governed more by diffusion than kinetics in this case. Overall, these results for several cases confirmed that the code was working properly.

Parametric Results for Linear Pressure-Coupled Response

Linear pressure-coupled response function curves were computed numerically from the amplitudes and phases of the burning rates following several cycles of oscillations to assure equilibrium. The absolute values and real and imaginary parts were examined for each ingredient and the aggregate propellant. The response function curves covered selected ranges of Ω at increments of 0.4 and, for the time steps used, a complete curve could be generated in about

Table 1 Steady-state model results 87% AP (20 μm), 68 atm, no crossflow

Parameters	Value	Parameters	Value	Parameters	Value
m_p	3.85 g/cm^2 · s	$m_{\rm ox}$	3.87 g/cm^2 · s	m_f	3.75 g/cm^2 · s
$S_{\rm ox}$	0.866	$T_{S{\rm ox}}$	919 K	T_{Sf}	1364 K
β_p	0.523	Q_L	−17.8 cal/g[a]	$Q_{\rm ox}$	440 cal/g
$\beta_{\rm ox}$	0.781	$Q_{\rm PF}$	1016 cal/g	β_F	1.00
$X^*_{\rm ox}$	7.16 μm	$X^*_{\rm PDF}$	2.04 μm	——	——

[a]Exothermic.

Table 2 Nonsteady model results 87% AP (20 μm), 68 atm, no crossflow[a]

P	m_p	$m_{\rm ox}$	m_f	$\alpha_{\rm ox}$	Q_L	$Q_{\rm ox}$	$Q_{\rm PF}$	$X^*_{\rm ox}$	$X^*_{\rm PDF}$
1.0000	3.8536	3.8694	3.7508	0.870000	−17.7792	440.397	1016.428	7.164	2.0354
1.0016	3.8548	3.8705	3.7525	0.869980	−17.7740	440.407	1016.413	7.143	2.0348
1.0031	3.8563	3.8720	3.7544	0.869966	−17.7667	440.418	1016.406	7.123	2.0342
1.0045	3.8578	3.8734	3.7561	0.869956	−17.7593	440.430	1016.405	7.104	2.0337
1.0059	3.8592	3.8748	3.7577	0.869948	−17.7523	440.441	1016.406	7.087	2.0332
1.0071	3.8604	3.8760	3.7591	0.869943	−17.7459	440.451	1016.410	7.072	2.0328
1.0081	3.8615	3.8771	3.7602	0.869939	−17.7405	440.459	1016.416	7.059	2.0324
1.0089	3.8623	3.8779	3.7611	0.869938	−17.7361	440.466	1016.422	7.049	2.0321
1.0095	3.8629	3.8785	3.7617	0.869938	−17.7329	440.471	1016.429	7.041	2.0319
1.0099	3.8633	3.8789	3.7620	0.869941	−17.7309	440.474	1016.437	7.037	2.0318
1.0100	3.8634	3.8791	3.7620	0.869944	−17.7301	440.475	1016.444	7.035	2.0317
1.0099	3.8633	3.8789	3.7617	0.869949	−17.7307	440.474	1016.451	7.037	2.0318
1.0095	3.8629	3.8786	3.7611	0.869956	−17.7326	440.471	1016.457	7.041	2.0319
1.0089	3.8623	3.8780	3.7603	0.869963	−17.7357	440.466	1016.463	7.049	2.0321
1.0081	3.8614	3.8772	3.7592	0.869972	−17.7400	440.459	1016.468	7.059	2.0324
1.0071	3.8603	3.8761	3.7579	0.869981	−17.7453	440.451	1016.471	7.072	2.0328
1.0059	3.8591	3.8749	3.7564	0.869990	−17.7515	440.442	1016.474	7.087	2.0332
1.0045	3.8577	3.8735	3.7548	0.870000	−17.7585	440.431	1016.476	7.104	2.0337
1.0031	3.8562	3.8721	3.7530	0.870009	−17.7662	440.419	1016.476	7.123	2.0342
1.0016	3.8546	3.8705	3.7512	0.870018	−17.7742	440.407	1016.474	7.143	2.0347

[a]Time increment equal to period/40, half-wave, for $\Omega_{\rm ox} = 7.0$.

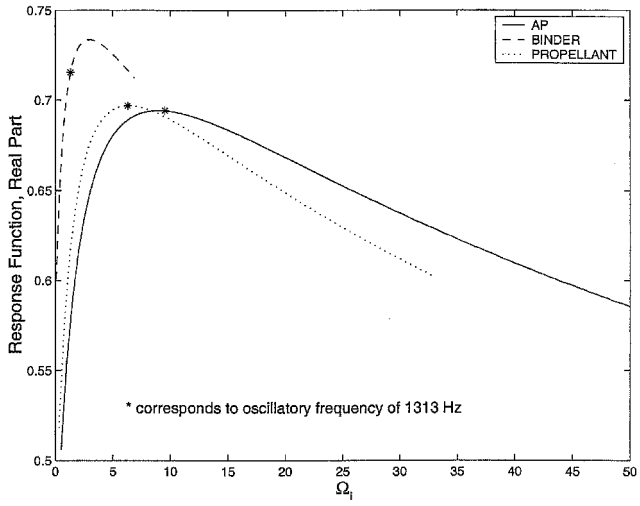

Fig. 1 Computations of real parts of pressure-coupled response functions vs their respective dimensionless frequencies for AP, binder, and the aggregate propellant: 87% AP (20 μm)/HTPB binder at 27 atm, 298 K, and 0 m/s crossflow.

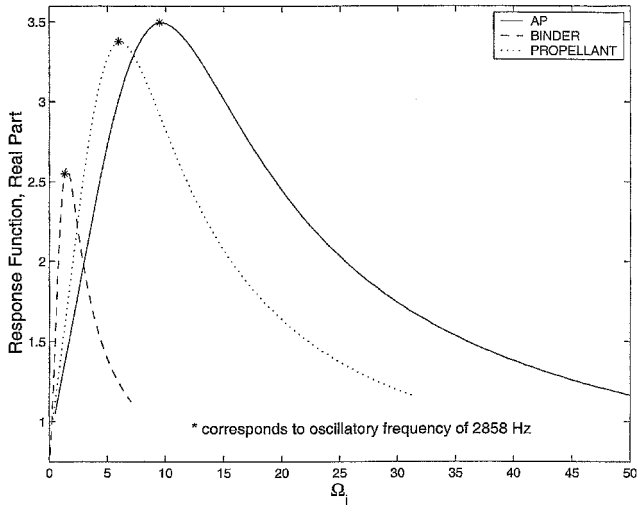

Fig. 2 Computations of real parts of pressure-coupled response functions vs their respective dimensionless frequencies for AP, binder, and the aggregate propellant: 87% AP (90 μm)/HTPB binder at 170 atm, 298 K, and 0 m/s crossflow.

2 h on a personal computer (about 2 min per frequency). Examples of results are shown in Figs. 1 and 2.

Figure 1 is for 20-μm AP at 27 atm (~2.7 MPa), a pressure that is of interest as a possible sustain pressure in a boost–sustain motor application. Note the separate curves for binder, AP, and the aggregate propellant. The Ω are for each ingredient and for the propellant at a given dimensional frequency (hertz). For clarity, a specified dimensional frequency is starred on each curve to show where the Ω are located for that frequency. Note that the binder is phase leading at that frequency (on the left of its peak), the AP is slightly phase lagging, and the propellant is in phase with the pressure. Also, note that the peak response of the binder is higher than that of the AP at this condition. The peak responses are relatively low, reflecting the diffusion control.

There is no indication of a dual-peaked response function curve arising from the two-component system. Perhaps this is because the phase differences between AP and binder are not large and the binder contributes a minor portion of the mass flow. Thus, we need to return to the idea that AP size modalities are the basis for dual (or more) peaks, unless a different model can show such gross phase differences between the AP and binder as to overcome the small mass flow contribution from the binder.

Table 3 Effect of AP size and pressure on peak of pressure-coupled response function of aggregate propellant, 87% AP

Pressure, atm	Peak R_{pc}	Ω_p at peak	Frequency at peak, Hz
	2-μm AP		
27	1.22	5.96	2800
68	1.13	5.62	13500
150	0.93	5.52	43600
170	0.88	5.53	51200
	20-μm AP		
27	0.69	6.16	1300
68	0.28	5.98	2400
150	1.45	7.03	6300
170	1.52	7.07	7100
	90-μm AP		
27	1.28	7.14	310
68	1.65	6.78	940
150	2.69	6.07	2500
170	3.37	5.89	2900
	200-μm AP		
27	1.48	6.33	180
68	2.21	5.98	610
130	6.82	5.47	1300
150	14.9	5.48	1600
170	——[a]	——[a]	——[a]

[a]Intrinsically unstable.

Figure 2 is for 90-μm AP at 170 atm (~17.0 MPa), which would correspond to a boost or high-performance pressure. Here, the peak response of the binder is less than that of the AP. The dimensional frequency selected to highlight the Ω differences here show a slight phase lead for the binder while the AP and propellant are in phase with the pressure. The peak responses are higher than in Fig. 1, reflecting the greater influence of the AP flame with the coarser AP at the higher pressure, and the curves are more peaked in appearance.

Highlights of propellant results for four AP particle sizes at several pressures are summarized in Table 3. The peak values of the propellant response and the frequencies at which they occur are shown.

Peak response Ω_p falls in the range 5.5–7.1, showing that the surface decomposition parameters that contribute to combustion response are not changing very much over a broad range of conditions. In general, this Ω appears to first decrease with increasing pressure, due to the increases in surface temperatures, but then it levels off or eventually increases with pressure at higher pressures. The most pronounced example of this change in trend is with 20-μm AP, perhaps because its stronger shift from diffusion flame control to AP flame control at higher pressure has a larger effect on the mix of AP and binder contributions.

The changes in dimensional peak response frequency are of more practical interest and are very large. Because the Ω_p are within narrow bounds, the dimensional frequency is mainly a function of the square of the mean burning rate in accordance with the characteristic response time. Coarse AP with its attendant lower burning rate is more responsive to low frequencies, of the order of hundreds of hertz, which correspond to the axial modes of many motors of interest. Fine AP, on the other hand, is more responsive to high frequencies (thousands or tens of thousands of hertz), which correspond to tangential modes and harmonics of the various modes in motors of interest. However, frequencies of order of thousands of hertz violate the quasi-steady gas-phase assumption. Higher pressures also shift the peak response frequencies to higher values.

Peak response magnitudes are primarily affected by the pressure exponent and secondarily by the nature of the heat feedback law, namely, the mix of mechanisms in the energy balance or boundary condition. Trends with AP particle size depend on pressure, and trends with pressure depend on particle size, a result of the changing flame structure (the AP flame vis-à-vis the diffusion flame and kinetics vs diffusion). These have been discussed in many earlier

papers and the results here are in agreement with them. The peak response minimizes at a combination of AP size and pressure, where diffusion control is maximal and the pressure exponent minimizes, roughly 20 μm at 68 atm. The peak response is largest where the AP as a monopropellant dominates the combustion and the exponent approaches unity, with coarsest AP at highest pressures. It was not necessary to include 400-μm AP in the study to encounter an intrinsic instability. Note how the peak response increases rapidly with pressure at high pressure for 200-μm AP. This important result will be discussed further subsequently. Where response functions become large, the nature of the heat feedback law is more important than the pressure exponent.

The peak response of coarse AP corresponds to axial mode frequencies, whereas the peak response of fine AP corresponds to tangential mode frequencies. It is for this reason that the rule of thumb is that coarse AP drives axial modes and fine AP drives tangential modes. The higher losses of the axial modes compared to the tangential modes, which are present due to nozzle damping, are overcome by the higher peak responses of the coarse AP compared to the fine AP.

Remarks on Intrinsic Instability and Modeling Implications

An intrinsic instability was encountered for the case of 200-μm AP at 170 atm. The rapidly increasing peak responses at 130 and 150 atm show the approach to this condition. The intrinsic instability is manifested numerically by a divergence between the energy dissipation from gasification and the heat feedback law, such that the surface temperature cannot converge no matter how small the perturbation amplitude or time step. The culprit is the AP, under such conditions where the combustion of the AP in the propellant is dominated by its own monopropellant process (coarse AP at sufficiently high pressure). The steady-state results showed that the role of the diffusion flame was insignificant here, providing a very small fraction of the heat feedback to the AP surface ($\beta_F = 0.016$). A computer experiment was performed, making $\beta_F = 0.3$ by overriding the code. Stable oscillations were achieved, showing the stabilizing influence of the diffusion flame under conditions where the AP would be unstable by itself.

The recent paper by the authors on the combustion response properties of monopropellant AP (Ref. 7) devoted significant space to intrinsic instability. It comes about when the combustion is totally dominated by condensed-phase exothermicity at low pressure or when the flame height becomes vanishingly small at high pressure. Either way, it can be thought of as a heat release at the surface which, from a dynamic stability standpoint, is like balancing a pyramid on its point. It was shown that the model does predict intrinsic instability limits at extremes of high and low pressure, but apparently not at the correct pressures. The data of Finlinson et al.[8] for AP indicate that the peak response functions may be increasing as these low- and high-pressure limits are approached, but more data are needed to make closer approaches to confirm that.

The prediction of an intrinsic instability for the propellant raises a serious question about the correctness of the steady-state model in describing bimodal or trimodal propellants. Of course, the steady-state model can predict a burn rate because there is no dynamic mechanism, and there is no such thing as an 87% monomodal AP propellant to test. The real question is, what stabilizes the 200-μm AP in real bimodal or trimodal propellants at very high pressures if it would be intrinsically unstable as computed here? The answer lies in a better description of the diffusion flame. The present model uses the interstitial spacing between the 200-μm AP in the characteristic dimension for the diffusion length, whether the propellant is monomodal or bimodal. This has the potential for yielding a β_F that is too low. It appears that a more correct approach would be to account for the presence of the fine AP in surrounding the coarse AP and thus derive a shorter characteristic length to operate around the periphery of the coarse AP. Such a rederived model has the potential to increase the β_F for the coarse AP and, thus, stabilize it as was shown in the computer experiment described earlier. This would be recommended for any future modeling work involving bimodal propellants.

Comparison with Response Function Data

The most extensively tested propellant for response functions is A-13, a research formulation consisting of 76% AP (nominal 90 μm) in polybutadiene-acrylonitrile binder. For purposes of the model, it is a monomodal AP propellant, and the values for the binder input parameters are known. Data were obtained at many different facilities as part of a JANNAF workshop[18] and for other research.[19–21] Coauthor Cohen has retained considerable data for A-13 in his files and Beckstead and Meredith[22] have published a recent review. These data were used to construct a composite plot that the model could be compared to.

Files of particle size distributions that were used in A-13 show actual weight-mean diameters ranging from 65 to 85 μm. Burning rates over the range 14.6–21.4 atm, where most of the data were obtained, showed a spread of 14% from several sources. This is about equal to the difference in the burning rates at these two pressures. The pressure exponents were in much better agreement. In view of these discrepancies, it was decided to combine and compare all of the response function data over this pressure range on a single plot. No pressure effect could be discerned from the scatter in the data. Model computations performed with 65-, 75-, and 90-μm AP did not show significant differences.

The composite plot of the data together with a model prediction (using 75 μm AP at 21.4 atm) is shown in Fig. 3. A discussion of the data scatter was included in Beckstead and Meredith's recent review paper[22] and need not be repeated here. Note that the response function reaches relatively high peak values, a credible result shown by several sources, and that the model is unable to predict it. However, the model provides a very good fit of the data at frequencies above an Ω_p of 35.

This deficiency of the model at low pressure is related to its incorrect prediction of the low-pressure limit for AP (Ref. 7). When it is assumed that the low-pressure deflagration limit of monopropellant AP (about 13 atm) is caused by intrinsic instability, the model does not predict this to occur until subatmospheric pressure. The approach to intrinsic instability is reflected by a decrease in the B parameter (temperature sensitivity of the heat feedback law) of classical theory, which sharpens the response function curve and increases the peak value. It was speculated that there might be a change in mechanism at low pressures to explain this deficiency in the model. This was tested by another computer experiment in which the relative importance of the flame was artificially reduced

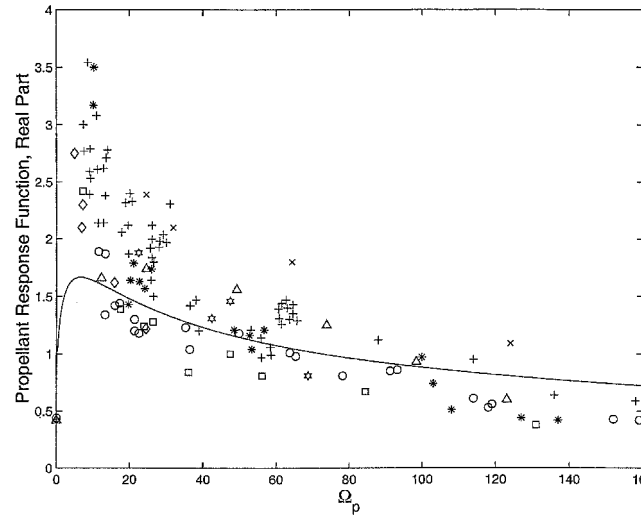

Fig. 3 Comparison of model calculations with composite data from many sources[18–22] for A-13 propellant, real part of the pressure-coupled response function vs dimensionless frequency. Computations for 76% AP (75 μm)/PBAN binder at 21.4 atm, data for 76% AP (65–85 μm)/PBAN binder at 14.6–21.4 atm: +, California Institute of Technology; □, Lockheed; ◇, Jet Propulsion Laboratory; △, Naval Weapons Center; ○, University of Utah; ∗, United Technologies; ⋆, Rocketdyne; and ×, Naval Weapons Center.

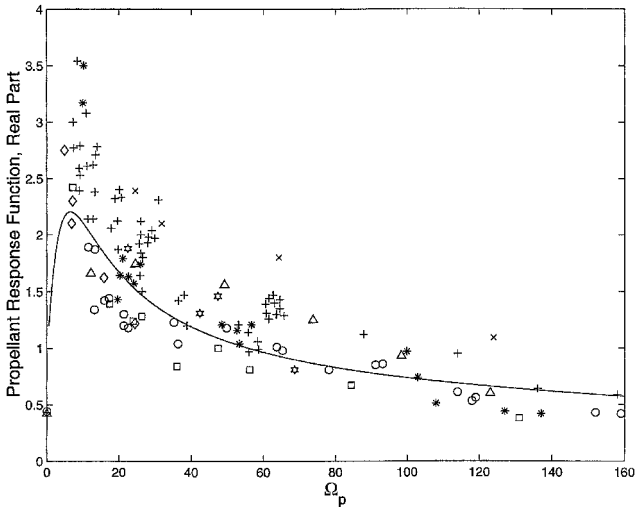

Fig. 4 Repeat of Fig. 3 with arbitrary increase in the flame height imposed on the model.

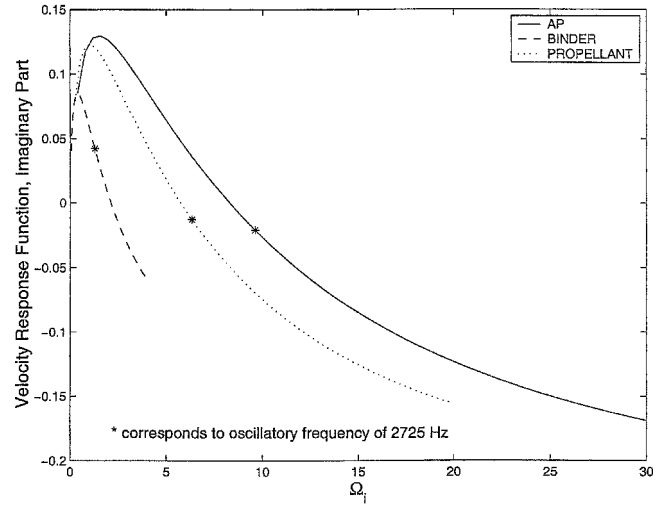

Fig. 5 Computations of imaginary parts of velocity-coupled response functions vs their respective dimensionless frequencies for AP, binder, and the aggregate propellant: 87% AP (20 μm)/HTPB binder at 68 atm, 298 K, and 120-m/s crossflow speed.

to simulate such a change. The result, plotted in Fig. 4, shows that this is in the right direction.

Data for other monomodal AP research formulations, for example, UTX-8501 (Ref. 23), also show high values of peak response at low pressure. Therefore, high response is not limited to A-13. UTX-8501 contained 78% of 180-μm AP in carboxyl-terminated-polybutadiene binder, and the data were at 14.6 atm. The peak values were even higher than those for A-13, which may be due to the coarser AP size. The mechanism responsible for this low-pressure behavior would be accentuated by larger AP particle size because coarser AP in propellants behaves more like monopropellant AP.

Although most of these early T-burner data with research-type propellants were acquired at low pressures, there are some data at higher pressures and Beckstead and Meredith[22] pointed out that the peak response decreases with increasing pressure above 14 atm. For example, Ibiricu[21] showed peak values at 28–55 atm in a range that would be predicted by the model (peak values between 1.0 and 2.5). Unfortunately, Ibiricu plotted curve fits rather than data so that the number of points or their scatter are unknown. Beckstead and Meredith[22] also noted that the responses of practical propellants at pressures of interest are in this lower range. Future modeling will have to resolve the inaccuracy at low pressure vis-à-vis the higher pressures where the model appears to be satisfactory.

Crossflow Effects and Velocity-Coupled Response

Including crossflow affects the pressure-coupled response, as well as the mean burning rate, via the erosive burning mechanism. In general, velocity fluctuations accompany the pressure perturbations, but it is possible to locate a propellant sample in a standing wave where there are no velocity fluctuations, for example, the ends of a T-burner or motor experiencing an axial mode. A series of computations were made to include various mean crossflow speeds in computing the pressure-coupled response. Results were consistent with previous findings.[6] Basically, a mean crossflow has a small effect on the peak value of the response. The main effect is to increase the dimensional frequency of the peak response because of the increase in the mean burning rate.

The next check of the code was to compute velocity-coupled response functions with various mean crossflow speeds at constant pressures. [Note that velocity-coupled response was defined as $R_{vc} = (R-1)(a/u')$.] This simulates a propellant placed in the middle of a T-burner or motor experiencing an axial mode. Note that the concept of velocity-coupled response has been controversial, and attempts to measure it have been viewed very skeptically. Thus, no comparisons with data will be made here. A result is shown in Fig. 5 for the standard case with a mean crossflow speed of 120 m/s. (For linear velocity coupling, the imaginary part is the relevant driving component.) For this case, the peak responses (phase-leading positive and phase-lagging negative) are comparable in magnitude to the peak pressure-coupled response (Table 3). Note that the binder is phase leading whereas the AP and aggregate propellant are phase lagging.

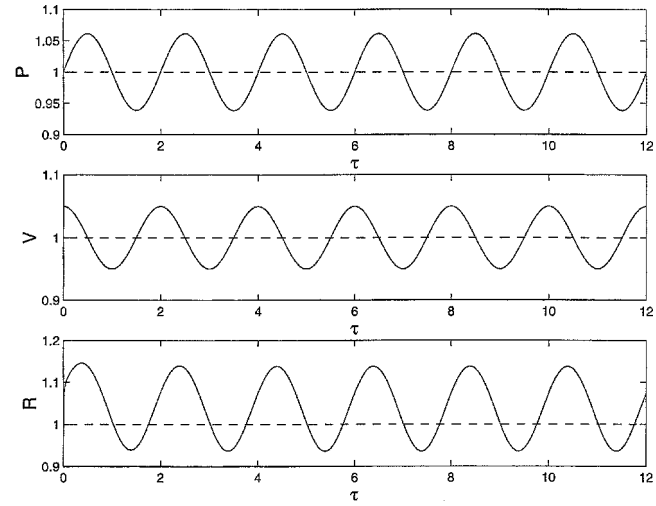

Fig. 6 Propellant combustion response to imposed standing wave: 87% AP (200 μm)/HTPB binder at 68 atm and 80-m/s crossflow speed; 5% velocity perturbation with corresponding pressure perturbation at $\Omega_{ox} = 3$.

Parametric effects were consistent with previous findings.[6] The important trends in the peak values of the velocity-coupled response function are that they tend to 1) increase with increasing AP particle size, 2) increase with increasing pressure, and 3) decrease with increasing mean crossflow speed. Thus, coarse AP and high pressure are aggravating to both pressure-coupled and velocity-coupled response functions at axial-mode frequencies, which have important motor stability implications for AP propellants that are consistent with motor experience.

Nonlinear Solutions

Examples of computed propellant responses to finite-amplitude waves are shown in Figs. 6 and 7. The AP particle size is 200 μ, pressure is 68 atm, and mean crossflow speed is 80 m/s. The first wave represents a standing wave with a velocity perturbation of 5% at $\Omega_{ox} = 3$. The second represents a traveling saw-toothed wave with a velocity amplitude of 20% at the same frequency. The propellant

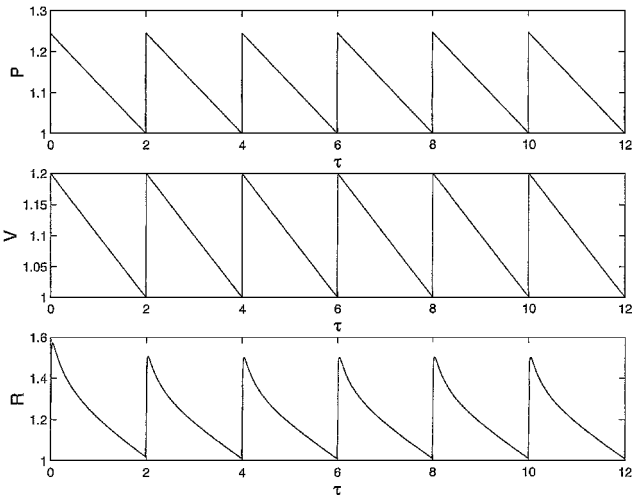

Fig. 7 Propellant combustion response to imposed traveling sawtooth wave: 87% AP (200 μm)/HTPB binder at 68 atm and 80-m/s crossflow speed; 20% velocity disturbance with corresponding pressure amplitude at $\Omega_{ox} = 3$.

is located at the quarter-wave point of a standing axial mode, and the combustion responds to both the pressure and velocity.

Figure 6 shows that the combustion response is sinusoidal, but there is a small dc shift owing to the acoustic erosivity. Note that the combustion wave leads the pressure and lags the velocity. The combustion response is larger than the pressure and velocity amplitudes, but does not feed back to the gasdynamics, and so the imposed waves do not change. Figure 7 simulates a steepened wave to a traveling sawtooth, whereby the pressure and velocity are now in phase. The combustion closely follows the wave behavior, and its dc shift is now pronounced owing to the nature of the wave. The flow speed of 80 m/s is always greater than the threshold speed of 44.7 m/s so that there is no distortion in the combustion response. (See Ref. 6 for the expression for the threshold velocity.) The response is, again, larger than the amplitudes of the imposed waves.

The small dc shift in Fig. 6 can contribute to the wave steepening process arising in the motor gasdynamics, which then feeds on itself by further augmenting the combustion response as in Fig. 7. Beddini's model (see Ref. 15) provides a mechanism for the combustion to drive the higher harmonic content of the steepened wave, something which previously had been represented in an ad-hoc way by Baum and Levine.[1]

Conclusions

An AP composite propellant model code for unsteady combustion has been developed and checked. It uses the Cohen and Strand[4] model for AP composite propellants as boundary conditions, one for AP and one for binder, in solving the heat conduction equation in each component to compute linear and nonlinear combustion response properties for both components and for the aggregate propellant. Iterations couple AP and binder through the quasi-steady flame processes.

The model contains mechanisms that are absent from the Baum and Levine[1] code, such as explicit effects of AP particle size on the combustion process and the frequency dependence of turbulence penetration of the combustion zone.

The code appears well suited to describe propellant effects in motors at conditions of practical interest. Computed trends are in reasonable agreement with rules of thumb gained from prior experience, and features of parametric results appear to behave smoothly.

The model predicts a very large peak response at high pressures with coarse AP due to AP monopropellant combustion, underpredicts peak response amplitude for low pressures due to a possible change in mechanism, and shows a stabilizing effect of the diffusion flame.

The instability of AP propellants is thought to be largely due to the instability properties of the AP, the presence of the binder, and the diffusion flame being stabilizing. This result has stimulated a purely mathematical derivation of the combustion response, which will be the subject of a separate paper.[25]

Future work needs to complete the coupling with the gasdynamics in the combustion chamber and then extend the capability to bimodal and trimodal AP propellants. When this extension is made to multimodal AP, some revisions in describing the diffusion flame appear to be necessary. Indeed, the community needs to come to some agreement on how the various particle size groupings contribute to nonsteady behavior. Continuing advancements in computer technology will make feasible multiple coupled solutions of the transient heat conduction equation, such as the recent calculations of Knott and Brewster[2] and Hegab et al.[3] There also needs to be more work on the low-pressure combustion response of AP, including more response function data at low pressures approaching its low-pressure limit.

Acknowledgments

This work is sponsored partly by the California Institute of Technology and partly by the Office of Naval Research under Grant N00014-95-I-1338. Judah Goldwasser is the Navy Program Manager.

References

[1]Baum, J. D., and Levine, J. N., "Modeling of Nonlinear Combustion Instability in Solid Propellant Rocket Motors," U.S. Air Force Research Lab., Rept. AFRPL-TR-83-058, Edwards AFB, CA, Feb. 1984.

[2]Knott, G. M., and Brewster, M. Q., "Two-Dimensional Combustion Modeling of Heterogeneous Solid Propellants with Finite Peclet Number," *Combustion and Flame*, Vol. 121, No. 1–2, 2000, pp. 91–106.

[3]Hegab, A., Jackson, T. L., Buckmaster, J., and Stewart, D. S., "Nonsteady Burning of Periodic Sandwich Propellants with Complete Coupling between the Solid and Gas Phases," *Combustion and Flame*, Vol. 125, No. 1–2, 2001, pp. 1055–1070.

[4]Cohen, N. S., and Strand, L. D., "An Improved Model for the Combustion of Ammonium Perchlorate Composite Propellants," *AIAA Journal*, Vol. 20, No. 12, 1982, pp. 1739–1746.

[5]Cohen, N. S., and Strand, L. D., "Combustion Response to Compositional Fluctuations," *AIAA Journal*, Vol. 23, No. 5, 1985, pp. 760–767.

[6]Cohen, N. S., and Strand, L. D., "Effect of Ammonium Perchlorate Particle Size on Combustion Response to Crossflow," *AIAA Journal*, Vol. 23, No. 5, 1985, pp. 776–780.

[7]Shusser, M., Culick, F. E. C., and Cohen, N. S., "Combustion Response of Ammonium Perchlorate Composite Propellants," *AIAA Journal*, Vol. 40, No. 4, 2002, pp. 722–730.

[8]Finlinson, J. C., Stalnaker, R. A., and Blomshield, F., "Ultrapure Ammonium Perchlorate T-Burner Pressure Coupled Response at 500, 1000, and 1800 psi," AIAA Paper 98-3554, July 1998.

[9]Beckstead, M. W., Derr, R. L., and Price, C. F., "A Model of Composite Solid-Propellant Combustion Based on Multiple Flames," *AIAA Journal*, Vol. 8, No. 12, 1970, pp. 2200–2207.

[10]King, M. K., "Erosive Burning of Composite Solid Propellants: Experimental and Modeling Studies," *Journal of Spacecraft and Rockets*, Vol. 16, No. 3, 1979, pp. 154–162.

[11]Beckstead, M. W., "Solid Propellant Combustion Mechanisms and Flame Structure," *Journal of Pure Applied Chemistry*, Vol. 65, No. 2, 1993, pp. 297–307.

[12]Cohen, N. S., "Effects of Formulation on the Combustion of Solid Propellants," Cohen Professional Services, Rept. AFAL-TR-88-090, Redlands, CA, Sept. 1988.

[13]Surzhikov, S. T., Murphy, J. J., and Krier, H., "Two-Dimensional Model for Unsteady Burning Heterogeneous Ammonium Perchlorate/Binder Solid Propellants," AIAA Paper 2000-3573, July 2000.

[14]King, M. K., "Composite Propellant Combustion Modeling," AIAA Paper 80-1124, July 1980.

[15]Cohen, N. S., Shusser, M., Culick, F. E. C., and Beddini, R. A., "Combustion Modeling of AP Composite Propellants for Stability Analysis," *36th JANNAF Combustion Meeting*, C.P.I.A. Publ. 621, Oct. 1999, pp. 597–608.

[16]Beckstead, M. W., "Combustion Calculations for Composite Solid Propellants," *13th JANNAF Combustion Meeting*, CPIA Publ. 281, Vol. 2, Chemical Propulsion Information Agency, Laurel, MD, 1976, pp. 299–312.

[17]Renie, J. P., Condon, J. A., and Osborn, J. R., "Oxidizer Size Distribution Effects on Propellant Combustion," *AIAA Journal*, Vol. 17, No. 8, 1979, pp. 877–883.

[18]Culick, F. E. C., "T-Burner Manual," CPIA Publ. 191, Chemical Propulsion Information Agency, Columbia, MD, 1969.

[19]Horton, M. D., "The Effect of Propellant Additives upon Oscillatory Combustion of Solid Rocket Propellants," Meeting of the Western States Section of the Combustion Inst., April 1963.

[20]Perry, E. H., "Investigation of the T-Burner and Its Role in Combustion Instability Studies," Ph.D. Thesis, Mechanical Engineering, California Inst. of Technology, Pasadena, CA, 1970.

[21]Ibiricu, M., "Experimental Studies on the Oscillatory Combustion of Solid Propellants," Naval Weapons Center, Rept. NWC-TP-4393, China Lake, CA, March 1969.

[22]Beckstead, M. W., and Meredith, K. V., "Examples of Unsteady Combustion in Nonmetalized Propellants," AIAA Paper 2000-3696, July 2000.

[23]Brown, R. S., and Muzzy, R. J., "Linear and Nonlinear Pressure Coupled Combustion Instability of Solid Propellants," *AIAA Journal*, Vol. 8, No. 8, 1970, pp. 1492–1500.